Nig. J. Biotech. Vol. 36 (2) : 167–187 (Dec 2019)
ISSN: 0189 1731
Available online at
http://www.ajol.info/index.php/njb/index
and www.biotechsocietynigeria.org
DOI: https://dx.doi.org/10.4314/njb.v36i2.17

NIGERIAN JOURNAL OF BIOTECHNOLOGY

Analysis of differentially expressed genes induced by drought stress in tef (*Eragrostistef*) root

Hewan Demissie Degu

Hawassa University College of Agriculture, School of Plant and Horticulture Science, Plant Biotechnology

Abstract

Drought stress is one of the major abiotic stresses which induces root growth in tef. Molecular mechanisms underlying the elongation of roots under drought stress are not known. Therefore, we aimed to study the tef root system to uncover the expression profiles for drought stress using Agilent gene chip of rice. One hundred seventy-five expressed genes were found to be differentially expressed after eight days of drought stress with *Eragrostis tef*- resistant genotype, Kaye Murri. The drought-responsive genes were isolated and classified into nine categories according to the functional roles in plant metabolic pathways, such as defense, signal transduction, cell wall fortification, oxidative stress, photosynthesis, development, cell maintenance, RNA binding, and unknown functions. The profiles of tef root genes, responsive to drought stress shared common identities with other expression profiles known to be elicited by diverse stresses, including pathogenesis, abiotic stress, and wounding. Well-known drought-related transcription factor-like, WRKY and bHLH were up-regulated. Cell transport-related regulators such as potassium transporter 22-like, auxin transporter-like protein 1, and wall-associated receptor kinase were also involved in the expression profile of tef root under drought stress. Their expression had enhanced the drought-responsive genes, which, have a direct role to maintain root growth under drought stress.

Key words: Drought, Genome, Microarray, Root, Tef
Corresponding authors contact: hewan.dd@gmail.com; Tel.: +251-932243391

Introduction

Drought stress has been reported as one of the serious threats to staple crops, including *Eragrostis tef* (Abraha *et al*., 2016). It causes tremendous economic losses in tef production to the amount of approximately $21.3 million annually in Ethiopia. Drought basically affects the growth of root, which limits nutrient and water absorption. Therefore, researches that help to understand the mechanism of root elongation under drought stress have got increased attentions in order to breed crop plants that cope up drought stresses.

Due to its allotetraploid chromosome structure, tef is one of the least plastic plant species in terms of adaptation. However, the plant is capable of growing at high and low altitudes in tropical and subtropical climates. *Eragrostistef* plant has acquired a myriad of developmental and metabolic strategies to optimize water uptake. It also efficiently balances this with water utilization during vegetative growth and reproduction (Haile sillasie *et al*., 2016).

In the past, a few researches have been done to unravel the molecular processes of drought-induced regulations of tef root (Abraha et al.,

2016; Admas and Belay, 2011; Assefa *et al.*, 2011; Belay et al., 2008, 2009). Studies on shoot physiologyhave shown that sugars, sugar alcohols, amino acids, and amines function as osmolytes, protecting cellular functions from the effects of dehydration, and are known to accumulate under drought stress (Ayele, 1999 and Degu *et al.* 2008). Reduction in vegetative growth, stomatal closure and a decrease in the rate of photosynthesis (Admas and Belay 2011; Degu *et al.* 2008) are among the earliest responses of tef to drought, protecting the plant from extensive water loss.

Researchers have also identified that there are extensive genetic diversities in the physiological and root length of tef. This genetic variability has been exploited to produce locally adapted drought-tolerant tef cultivars for the dry tropical areas of Ethiopia (Plaza et al., 2013). The morphology of tef primary root and elongation at low water potentials have been studied (Degu *et al.* 2008) and QTL's affecting root length mapped (Degu and Fujimura, 2010). However, the expression patterns of root growth to water-deficit have not been sufficiently characterized.

Currently, plant science has entered a new era following the completion of the entire genomic sequence of Arabidopsis and rice (*Oryzasativa*). Researchers are using model plants to identify the specific functions of plant genes and their expression profiles. The genome, transcriptome, proteome and metabolome tools are used to analyze root system. The result of the transcriptome analysis vary based on the experimental setups, the different germplasm, and accessions used. Thus, there are different transcripts which describe the response of plant roots towards drought stress.

Focusing on tef, one transcriptome characterizations of tef plant in response to 1-week of drought showed 23 and 15 differentially expressed transcriptome (Cannarozzi *et al.*, 2014). The study suggests changes in energy (B-glucanase and ERD), salt-sensitive enzymes (SAL1) and chloroplast regulation (stay-green gene -SGR). This implies that there is a need to study how the root is regulated, and to understand the different transcriptome changes which contributed to the growth and elongation of root length under drought stress.

Rice is a model cereal crop to study the stress response at a molecular level due to the availability of whole-genome information and other molecular tools. Tef is one of the most drought-tolerant cereals, providing a useful platform to understand tolerance mechanisms. Besides, the genome of monocots are characterized by high synteny, and it is feasible to use rice chips to do hybridization with tef RNAs. In the present work, genome-wide transcriptional characterization of tef roots in response to drought deficiency is presented.

Identifying drought-responsive genes in the root, and the understanding of their function can lead to a better breeding of crop plants under drought stress. We applied microarray platforms to identify candidate genes that are associated with a phenotype of drought resistance in tef. The work plan applied the existing rice microarray technology created by the National Agricultural Research Organization of Ethiopia , and tests the feasibility of the orthologou arrays for use in multiple crops. The proposed project will enhance knowledge towards the elucidation of gene function in seminal root elongation under drought stress. Thus, the present study was planned to make a comparative study of drought responsiveness in drought and well-irrigated tef exploring the availability of whole-genome level information and molecular tools in rice.

Materials and Methods

Plant Material and Growth Conditions

The late-maturing improved variety of tef cv. Kaye Murre was used in the study. KayeMurre is capable of elongating its roots under drought stress (Degu and Fujimura, 2010). The seeds were obtained from Debreziet Agricultural Research center of Ethiopia. The seeds were surface sterilized and germinated on filter paper at 25°C in the dark. After 3 days, seedlings with seminal roots about 1 cm long were transplanted to a plastic root box (30 cm in width; 25 cm in diameter and 24 cm in height) containing (1) horticulture nursery soil (Kureha Ltd., Tokyo, Japan); with holes at the bottom. Horticulture nursery soil was porous, consisting of uniformly sized soil particles (0.5–3.0 mm), and containing0.4 g kg-1 of nitrogen, 1.9 g kg-1

of phosphorus, 0.6 g kg-1 of potassium, and 0.2 g kg-1 of magnesium. The liquid fertilizer was composed of nitrogen: phosphorus: potassium at the rate of 2:1:1.The growth conditions were 12/12 h day/night, one light period supplied 820 µmm-2s- photosynthetically active photon flux density (PPDF), 30/20°C (day/night); and temperature with RH 60 to 70%. For the control experiment, plastic root boxes were placed in tanks for a continuous supply of water through the root system. However, for drought stress treatment, root boxes were kept on a separate tank without the supply of water.

Soil, root and leaf water content measurement

Gravimetric soil water content was determined as described by Singh, &Baghini (2014). A soil sample was taken from three points within the plastic basket (both sides and a center) with a borer, and the collected soil was stored in a 1.5-ml Eppendorf tube to equilibrate soil moisture for 2 h. The water content was measured by using electric balance before and after drying the soil in the oven for 48 hrs. The measurement was replicated three times, and the data were averaged. Soil, leaf and root water potential were measured by using a dew point micro voltmeter (model HR33T, WESCOR, Inc. Logan, UT). First, the soil sample was taken using a borer (5 mm in diameter). The collected soil was stored in 1.5 ml Eppendorf tube to equilibrate to the surrounding environment for 2 hrs. Similarly, root sample and leaf sample were taken and kept in 1.5 ml Eppendorf tube.

For relative water content (RWC), two leaves per plant were cut and stored in Eppendorf tube on ice. The fresh weight (FW) was measured following immersing it in double-distilled water (DDW) for 8 hours. This was followed by measuring the turgid weight (TW). The sample was then oven-dried for 24 hrs at 80^{o} centigrade, and dry weight (DW) was measured after cooling it to 50 centigrade. RWC is calculated using the following formula;

$$\mathrm{RWC} = \frac{\mathrm{FW} - \mathrm{DW}}{\mathrm{TW} - \mathrm{DW}} \mathrm{x100}$$

For osmotic potential (OP) measurement, leaf and root samples (about 1.5 cm) were collected at 0, 2, 4, 6 and 8 days after drought stress treatment, and were kept in Eppendorf tube at -20 ° centigrade. During measurement, the samples were withdrawn from -20 ° centigrade and left at the room temperature to thaw. The Eppendorf was centrifuged at 14000 g for 15 minutes. The sap was measured by a dew point micro voltmeter (model HR33T, WESCOR, Inc.). Osmotic adjustment (OA) was calculated as the difference between the measured and expected concentration-effect OP of the drought stressed plants. For analysis of the transcription under drought stress, seminal root tips (1 cm) were harvested after 8 days of drought stress from the well-irrigated and drought-stressed sample. All samples were collected at noon. After harvesting, samples were immediately placed in liquid nitrogen and stored at −80°C until RNA extraction.

MicroArray experiments

The Microarray experiment was done following the standard procedure (Figure 1). Total RNAs were extracted from tef root using the RNeasy Maxi kit (Qiagen, Valencia, CA, USA). The RNA samples were treated with DNase I (NipponGene, Chiyoda-ku, Tokyo, Japan) and quantified by spectrophotometer using Nano Drop™ 1000 Thermo Scientific. The RNA quality was checked using the Agilent BioAnalyzer. Next, poly (A) + RNA was isolated from 200 µg of total RNA using an mRNA isolation system (Nippon- Gene, Japan). Linear amplification and labeling were carried out with fluorescent linear amplification kit (Agilent). Transcriptional analysis was carried out using a 22 mer-oligo chip from the Agilent Technologies produced by the Plant Functional Genomics Center, National Institute of Agricultural Science of Japan. The chip (Catalogue array- GA4138A) carries 21,000 genes from the genome of Oryza sativa L. spp. Japonica (Nipponbarre). Redundant probes were randomly distributed in triplicate across the array, each comprising a 22-mer oligonucleotide designed using inkjet-based technology which prints DNA on 1X 3" glass slide. The source of sequence information included a range of genes that can measure the expression of drought, salt and cold stress genes for rice and related plants(Sato *et al*., 2013). A complete description of the chip is available at the Rice Expression Profile Database (RiceXPro). Three biological replicates per treatment were analyzed. Four (4) microgram of labeled cDNA was hybridized to

the array according to the manufacturer's recommendations (Maruyama *et al*., 2014). The array was scanned with the Agilent DNA microarray scanner, and the expression data were extracted with the Agilent Feature Extraction software.

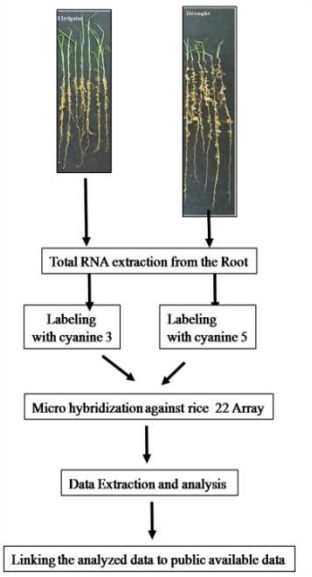

Figure 1. Experimental set up and hybridization of rice microarray on tef cDNA.

RT-PCR

Aliquot of total RNAs 10 µg RNA was reverse transcribed and used to synthesize single-stranded cDNA using the First-strand cDNA synthesis kit (TAKARA SHUZO CO. LTD., Otsu, Shiga, Japan) according to the manufacturer's instructions. RT-PCR reactions were performed with the Access RT-PCR kit (Thermo Fisher Scientific Inc) according to the manufacturer's protocol. The sequences of the primer were (FW=CGAGCGCTCCAACTCATC and RW= CAGCACCGAGCTGTCCTC with annealing temperature 60˚C. The amplicon size was 500 bp); WRKY gene fragments were then amplified using gene-specific primers. Gene expression patterns were normalized to the expression of the 18S ribosomal RNA (FW = AACGGCTACCACATCCAAGG , and RW = TCATTACTCCGATCCCGAAG). The PCR consisted of 40 cycles (30 s at 94 °C, 1 min at 60 °C, and 1 min at 72°C). The PCR-products were sequenced with (Macrogen, Korea).

Expression patterns of WRKY using real time-Quantitative-PCR

Quantitative PCR were carried out by designing primer using "Primer 3" software

(http://frodo.wi.mit.edu/primer3/) according to the following criteria: melting temperature: 59°C primers' length: 18-24 nucleotides, product size: 110 base pairs (bp) and GC content: 40-55%. Quantitative PCR was performed using cDNA made of 50 ng total RNA, with an Absolute QPCR SYBER Green ROX kit (Thermo Scientific, ABgene UK), using Rotor-Gene 6000 (Corbett life Sciences, Australia). Samples were first heated for 15 min. at 95°C followed by 40 PCR cycles of 10 s at 95°C, 15 s at 59°C and 20 s at 72 °C. Negative controls had no cDNA. Gene expression patterns were normalized to the expression of the QuantumRNA™ Classic 18S Internal Standard (Thermo Scientific, ABgene UK). The fold change is calculated according to the following formula.

$$\text{Ratio target gene in Drought Stress/Irrigated control} = \frac{\text{Fold change in target gene}}{\text{Fold change in Reference gene}}$$

Northern Blot Analysis

Root samples were harvested at mid-day in4, 6 and 8 days of drought-stressed sample, and were frozen in liquid nitrogen and then stored at –80°C until further use. Total RNAs were extracted using the RNeasy Maxi kit (Qiagen, Valencia, CA, USA). Samples were treated with DNase I (NipponGene, Chiyoda-ku, Tokyo, Japan) and quantified by spectrophotometer using Nano Drop™ 1000 Thermo Scientific. A 10µg aliquot of total RNA in a volume of 3.3µl was denatured by incubation with 1.5µl of 6 M glyoxal, 1.2µl of sodium phosphate buffer (0.1 M, pH 7.0) and 6µl of dimethylsulfoxide (DMSO) at 55°C for 1 h. The RNA solution was chilled on ice, and was separated by electrophoresis through a 1.2% agarose gel with 10 mM phosphate buffer. Afterwards, the RNA was transferred onto a Hybond N+ membrane (Amersham Biosciences), and was probed with [α-32P] dCTP-labeled DNA using the BCA Best labeling kit (Takara) according to the manufacturer's instructions in hybridization buffer [5× SSPE (SSPE is0.15 M NaCl, 10 mM sodium phosphate, 1 mM EDTA), 1× Denhalt'ssolution, 0.1% (w/v) SDS and 2 ng ml–1 DNA solutions from salmon sperm (Nippon gene)] for 24 h at 60°C. The blots were washed once in2× SSC (20× SSC is 3 M NaCl and 300 mM trisodium citrate) for 5 min at room temperature, once with 2× SSC, 0.1% (w/v) SDS for 15 min at 60°C, once with 1× SSC, 0.1% (w/v) SDS for 15 min at60°C and lastly with 0.1× SSC, 0.1% SDS (w/v) for 15 min at 60°C.Autoradiography was performed at –80°C using BioMax film (Kodak, Rochester, NY, USA) with an intensifying filter. The band intensities were quantified by using 'ImageJ' software (http://rsb.info.nih.gov/ij/)

Statistical Analysis

Analysis of variance and mean separation by Fisher's least significant difference methods were performed using Agricolae package with the statistical R programming language. Analysis of microarray raw data was performed using the open-source software of the Bioconductor project (Smyth *et al*., 2005) with the statistical R programming language (R Core Team 2018). Background adjustment, summarization and quintile normalization were performed using the limma package (Ritchie et al., 2015). Differentially expressed probes were identified by linear models' analysis (Ritchie *et al*., 2015) using limma package by applying Bayesian correction, an adjusted p-value of 0.05 and an absolute fold change |FC| ≥ 2. Functional annotation and physical location of the genes represented by the probe sets in the japonica genome were obtained from the Rice XPro website (McCouch, Symbolization, Linkage, & Cooperative, 2008). Genes were grouped into main functional categories according to the "biological" terms of the Gene Ontology (Mi *et al*., 2016) assigned to each rice EST (Release 12.0) based on the results of BlastP analysis against the UniProt database. Genes without significant BlastP results were classified as "Unknown"; Evalue < 1e-8; identity > 40%.

Results

Morphological change of tef root tip responding to drought stress

Drought stress induced the elongation of the seminal root in tef in accelerated fashion (Figure 2). The root lengths for plants placed under drought stress were33.3 % longer when compared to the well-irrigated sample. In terms of RWC and leaf water potential, there was no significant difference between drought-stressed and well-irrigated samples (Table 1). And the number of leaves were the same for both drought-stressed and well-irrigated control plants (Figure 2). The only difference was the shoot length, where there was accelerated plant height for irrigated control plants (Figure 3). However, there were significant differences between the two treatments in terms of soil and root water potential. Where the root water potential reduced to -1.2 MPa for drought-stressed sample, it remained -0.4 MPa for well-irrigated tef sample (Table 1). This indicates that when the drought stress increased, the available water content for the root was about 40% at field capacity. The available water content at field capacity was about 80% for well-irrigated control plants. This indicates clear water stress has been created in the drought-stressed sample.

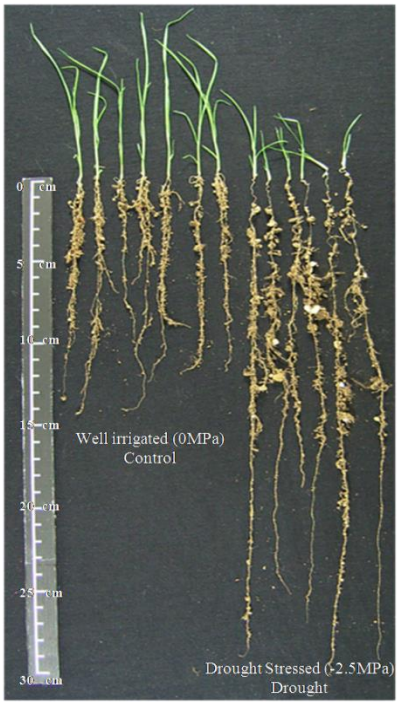

Figure 2. Shoot and root growth of E. tef at the indicated days after irrigation stopped . Root elongation of E. tef for the control (left) and drought (right) treatment at 0 and 2.5MPa of water potential.

However, OP for the drought-stressed plants was significantly lower than the well-irrigated control sample (Table 1). Specifically, the OA was the highest as the day for drought stress increases, and showed a significant difference between drought stressed and well irrigated samples. In the shoot, OA was the highest when compared to the root. The measured value was 0.05 MPa in control and 0.98 MPa in drought-stressed samples, respectively. It is important to note that compared to root under drought stress, the shoot exhibited lower OA, while the decrease in the RWC was significantly different, and it was the lowest for the root (Table 1).

Similarly, after 8 days of drought stress, the soil water potential for the control was about -0.5 MPa while it became -1.5 MPa under drought stress. Even though the soil water potential was significantly different between the control and stressed samples, the leaf water potential measurement and analysis showed no significant difference between the two treatments (Table 1). This was also confirmed by the non-significant difference between the two treatments on the relative water content. However, the root water potential was significantly different between the two treatments (Table 1). The effect of different water potential between the soil, root, and shoot was revealed on the shoot and root growth (Figure 2). Significant difference ($p \leq 0.05$) was observed for the shoot and root growth among the control and stressed plants of tef. Although there was a delay in the shoot growth under drought stress, seedlings maintained a healthy green color after 192 hrs of drought stress (Figure 2). On the other hand, there was no significant difference in leaf water potential for both control and drought-stressed plants. (Table 1).

Table 1. Relative water contents (RWC), osmotic potential (OP), and osmotic adjustment (OA) in shoot and root after stopping irrigation.

	Days after water withholding	Control			Stress		
		RWC(%)	OP (Mpa)	OA (Mpa)	RWC(%)	OP(Mpa)	OA(Mpa)
Shoot	0	97.6±0.86	0.90±0.07	0±0.04	98.5±0.64	0.87±0.1	0±0.04
	6	97.8±0.84	0.89±0.07	0.02±0.03	87.3±6.5	0.80±0.09	-0.07±0.08
	7	98.4±0.88	0.86±0.05	-0.02±0.03	93.8±6.5	0.85±0.08	-0.03±0.09
	8	97.4±0.83	0.80±0.05	-0.07±0.01	91.9±8.7	0.83±0.09	-0.04±0.06
	CV	4.9	6.7	-197.8			
	LSD	6.1	0.1	0.1			
Root	0	97.6±0.86	0.87±0.04	0±0	98.48±0.64	0.87±0.12	0±0
	6	97.8±0.83	0.89±0.11	0.02±0.04	84.02±2.9	0.39±0.1	-0.48±0.12
	7	98.4±0.88	0.75±0.15	-0.12±0.11	87.54±4.2	0.25±0.14	-0.61±0.1
	8	97.4±0.83	0.79±0.15	-0.07±0.14	86.06±3.4	0.31±0.24	-0.56±0.14
	CV	10.7	20.2	-52.8			
	LSD	12.8	0.2	0.2			

An asterisk represents a significantly greater value than the other accession at 5% (*), 1% (**) and 0.1%(***) level. The difference between accessions was statistically analyzed by Tukey pair wise comparison (ANOVA). A hyphen (-) indicates that all pieces of the three tested tissues were withered, and value in parenthesis indicates that 1–2 pieces of the three tested tissues were withered.

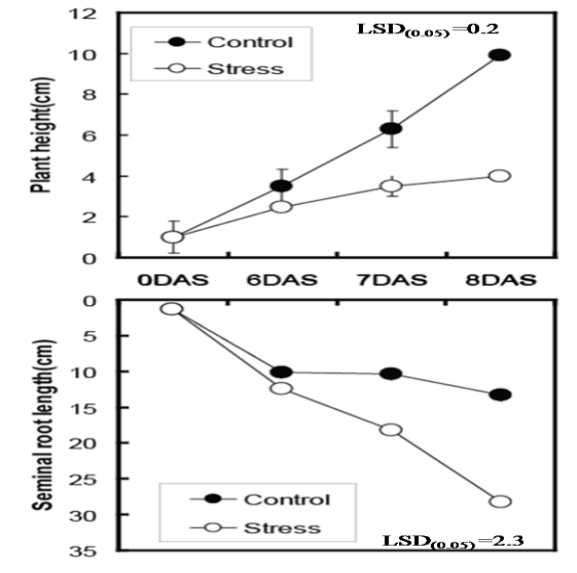

Figure 3. Influence of drought stress on leave and root growth of tef for 2,4, 6 and 8 days. Presented values for leaves and roots are the means of three replications. Vertical bars represent the SD.

Transcriptome analysis of tef root tips in response to drought

The drought-responsive genes were identified by changes in the gene expression patterns of the three replicates; the two-fold difference in the ratio of drought: control transcript abundance and *p-value* less than 0.05 (Figure 4, Table 2). The scatter plot of data from three replications to compare the control and stressed transcripts showed that there is a linear relationship between most of the genes expressed under control and stressed samples. From the 176 differentially expressed genes, 77 have greater than two-fold changes, but 93 genes were down-regulated with a fold change of less than or equal to minus two. Lesser number of genes were up and down-regulated might be due to the low hybridization signal because of low homology between orthologous genes.

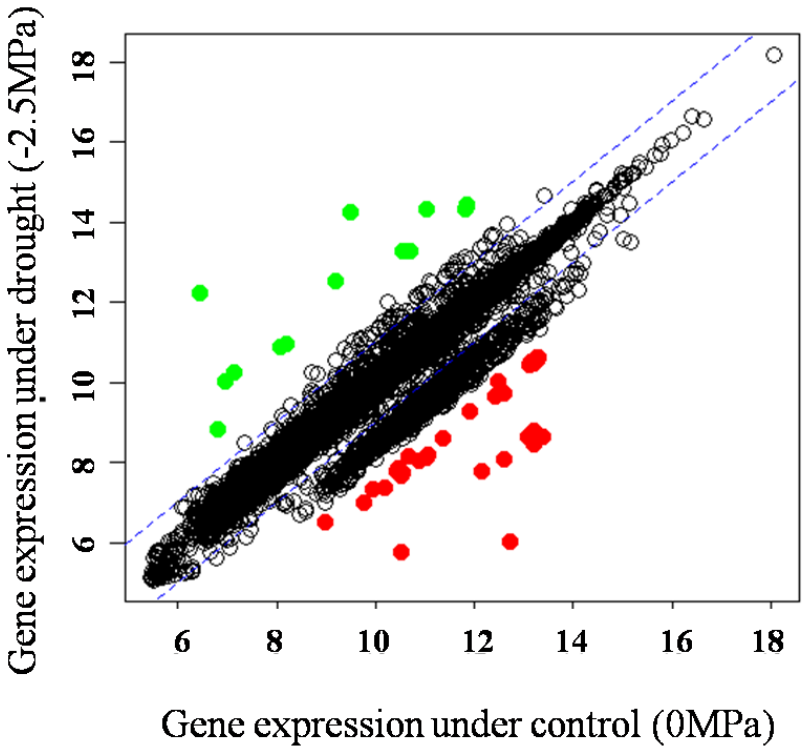

Figure 4. Scatter plot comparisons of microarray gene expression in drought-stressed E. tef . The normalized expression value (signal) for each gene under well-watered (control) vs. drought-stress plotted for E. tef at -2.5 MPa leaf water potential samples (A).

Table2. Selected drought responsive genes in *O sativa* highly hybridized resulted in up or down regulation of *E. tef* transcript (significant at 5% level)

ProbeName	GeneName|SystematicName	Gene symbol	Locus tag	Fold Change	-Log pval	Gene description
A_71_P120462	AK109080	LOC4344714	OSNPB_080159700	-4.8	4.2	AT-hook motif nuclear-localized protein 23
A_71_P113410	AK067302	LOC4333169	OSNPB_030428800	-4.4	4.9	Uncharacterized

A_71_P103875	AK058902	LOC4329688	OSNPB_02056240 0	-4.4	7.1	ankyrin repeat protein SKIP35
A_71_P126315	AK069006	LOC4352600	OSNPB_12057400 0	-2.9	4.7	beta-galactosidase 11-like
A_71_P120333	AK069943	LOC4344472	OSNPB_08010950 0	-2.9	4.7	(+)-neomenthol dehydrogenase
A_71_P110996	AK100257	LOC4337170	OSNPB_04064120 0	-2.9	4.7	Uncharacterized
A_71_P102759	AK102031	LOC4327316	OSNPB_01019460 0	-2.9	4.7	U-box domain-containing protein 11
A_71_P104162	AK102271	LOC4331143	OSNPB_02081680 0	-2.9	4.7	helicase-like transcription factor CHR28
A_71_P125325	AK102853	LOC4350717	OSNPB_11055560 0	-2.9	4.7	probable E3 ubiquitin-protein ligase BAH1-like 1
A_71_P102968	AK109457	LOC4324110	OSNPB_01068630 0	-2.9	4.7	probable calcium-binding protein CML27
A_71_P123735	AK109491	LOC4349090	OSNPB_10051050 0	-2.9	4.7	Uncharacterized
A_71_P126097	AK059940	LOC4352037	OSNPB_12040380 0	-2.9	4.6	probable receptor-like serine/threonine-protein kinase
A_71_P106066	AK063459	LOC4329297	OSNPB_02046120 0	-2.9	4.6	Uncharacterized
A_71_P126249	AK064505	LOC4351872	OSNPB_12024290 0	-2.9	4.6	Uncharacterized
A_71_P104593	AK067496	LOC4329918	OSNPB_02060550 0	-2.9	4.6	RINT1-like protein MAG2L
A_71_P106979	AK067772	LOC4330316	OSNPB_02067950 0	-2.9	4.6	Uncharacterized
A_71_P106439	AK102091	LOC4330628	OSNPB_02073220 0	-2.9	4.6	anamorsin homolog 1-like
A_71_P119754	AK103321	LOC4344573	OSNPB_08012780 0	-2.9	4.6	protein CDI
A_71_P122240	AK110546	LOC4347641	OSNPB_09052750 0	-2.9	4.6	Unknown expressed protein
A_71_P105146	AK058851	LOC4329525	OSNPB_02052720 0	-2.8	4.4	Uncharacterized
A_71_P118869	AK061900	LOC9270800	OSNPB_07051690 0	-2.8	4.4	50S ribosomal protein L31
A_71_P124449	AK063047	LOC4328135	OSNPB_02012310 0	-2.8	4.4	Unknown expressed protein
A_71_P114932	AK065359	LOC4339070	OSNPB_05047000 0	-2.8	4.4	glycine-rich RNA-binding protein 2, mitochondrial
A_71_P121233	AK066884	LOC4346328	OSNPB_08056160 0	-2.8	4.4	Uncharacterized
A_71_P109377	AK067103	LOC4331586	OSNPB_03014290 0	-2.8	4.4	50S ribosomal protein L28, chloroplastic
A_71_P125413	AK101774	LOC4350003	OSNPB_11019960 0	-2.8	4.4	indole-3-glycerol phosphate synthase, chloroplastic
A_71_P102782	AK108736	LOC4325031	OSNPB_01089920 0	-2.8	4.4	anaphase-promoting complex subunit 15
A_71_P102538	AK073493	LOC4325494	OSNPB_01076640 0	-2.7	4.8	fasciclin-like arabinogalactan protein 13
A_71_P121607	AK099503	LOC4347825	OSNPB_09055740	-	4.8	mitogen-activated protein kinase 14-

			0	2.7		like
A_71_P100151	AK100105	LOC4327103	OSNPB_01025100 0	-2.7	4.8	Protein trigalactosyldiacylglycerol 4, chloroplastic
A_71_P106899	AK100401	LOC4328582	OSNPB_02019210 0	-2.7	4.8	Uncharacterized
A_71_P115743	AK101156	LOC4340300	OSNPB_06017920 0	-2.7	4.8	Uncharacterized
A_71_P110642	AK103022	LOC4333590	OSNPB_03065090 0	-2.7	4.8	origin of replication complex subunit 1-like
A_71_P102476	AK112105	LOC9270556	OSNPB_01035420 0	-2.7	4.8	Unknown expressed protein
A_71_P103041	AK065358	LOC4324159	OSNPB_01073350 0	-2.7	4.8	protein trichome birefringence-like 28
A_71_P121864	AK068829	LOC4347892	OSNPB_09056800 0	-2.7	4.8	amino acid transporter AVT1C
A_71_P110380	AK069970	LOC4332513	OSNPB_03029280 0	-2.7	4.8	lachrymatory-factor synthase
A_71_P112428	AK101611	LOC4336833	OSNPB_04059270 0	-2.7	4.8	DNA annealing helicase and endonuclease ZRANB3
A_71_P102854	AK102203	LOC4324824	OSNPB_01085450 0	-2.7	4.8	NADH dehydrogenase [ubiquinone] 1 alpha subcomplex subunit 9, mitochondrial
A_71_P114265	AK103819	LOC4339464	OSNPB_05054010 0	-2.7	4.8	classical arabinogalactan protein 9
A_71_P103793	AK109718	LOC4327168	OSNPB_01065980 0	-2.7	4.8	glycosyl hydrolase 5 family protein
A_71_P103646	AK062051	LOC4326593	OSNPB_01063300 0	-2.7	4.4	non-specific lipid-transfer protein 2-like
A_71_P122572	AK068391	LOC4346642	OSNPB_09029400 0	-2.7	4.4	protein DETOXIFICATION 29
A_71_P115357	AK069632	LOC4337885	OSNPB_05016060 0	-2.7	4.4	Uncharacterized
A_71_P105946	AK072940	LOC4328666	OSNPB_02020370 0	-2.7	4.4	ubiquitin receptor RAD23d
A_71_P102743	AK100090	LOC4324749	OSNPB_01085650 0	-2.7	4.4	protein TRIGALACTOSYLDIACYLGLYCEROL 4, chloroplastic
A_71_P114270	AK103672	LOC4339458	OSNPB_05053950 0	-2.7	4.4	flap endonuclease 1-A-like
A_71_P127945	AK110168	LOC4326544	OSNPB_01074220 0	-2.7	4.4	Filobasidiellaneoformans var. neoformans translation elongation factor 2
A_71_P128119	AK110386	LOC4329433	OSNPB_02050490 0	-2.7	4.4	F-box/kelch-repeat protein At1g67480
A_71_P125176	AK064740	LOC4350576	OSNPB_11051280 0	-2.7	4.4	glutamine--tRNA ligase
A_71_P108336	AK066383	LOC9266989	OSNPB_03010005 0	-2.7	4.4	SCAR-like protein 1
A_71_P119552	AK066544	LOC4342173	OSNPB_07010210 0	-2.7	4.4	F-box/kelch-repeat protein At1g74510
A_71_P117169	AK073271	LOC4340699	OSNPB_06026430 0	-2.7	4.4	protein transport protein Sec24C
A_71_P111395	AK101488	LOC4334912	OSNPB_04010630	-	4.4	disease resistance protein PIK6-NP-

			0	2.7		like
A_71_P110635	AK105583	LOC4333158	OSNPB_03042590 0	-2.7	4.4	eukaryotic translation initiation factor 2 subunit alpha homolog
A_71_P112010	AK109273	LOC10727872 8	OSNPB_04065540 0	-2.7	4.4	ubiquitin-like modifier-activating enzyme 5
A_71_P109593	AK109470	LOC4332731	OSNPB_03033170 0	-2.7	4.4	auxin-responsive protein SAUR32
A_71_P102642	AK059715	LOC4324964	OSNPB_01089460 0	-2.7	4.7	Uncharacterized
A_71_P105802	AK063438	LOC4328135	OSNPB_02012310 0	-2.7	4.7	Uncharacterized
A_71_P126815	AK068049	LOC4351356	OSNPB_12012100 0	-2.7	4.7	glucose-6-phosphate isomerase 1, chloroplastic
A_71_P123898	AK070579	LOC4348282	OSNPB_10020970 0	-2.7	4.7	Uncharacterized
A_71_P111111	AK101835	LOC4336102	OSNPB_04046770 0	-2.7	4.7	G-type lectin S-receptor-like serine/threonine-protein kinase
A_71_P116173	AK102365	LOC4342018	OSNPB_06070810 0	-2.7	4.7	wall-associated receptor kinase 1
A_71_P112259	AK062775	LOC4333169	OSNPB_03042880 0	-2.7	4.3	protein CHAPERONE-LIKE PROTEIN OF POR1
A_71_P106457	AK064402	LOC4329874	OSNPB_02059820 0	-2.7	4.3	Uncharacterized
A_71_P117853	AK067620	LOC4344339	OSNPB_07068670 0	-2.7	4.3	chloroplastic import inner membrane translocase subunit HP30-2
A_71_P111034	AK102124	LOC4337380	OSNPB_04067440 0	-2.7	4.3	WUSCHEL-related homeobox 9-like
A_71_P119970	AK103306	LOC4346187	OSNPB_08054040 0	-2.7	4.3	Uncharacterized
A_71_P117941	AK106266	LOC4342464	OSNPB_07016290 0	-2.7	4.3	Uncharacterized
A_71_P117316	AK109313	LOC4329438	OSNPB_02050650 0	-2.7	4.3	ubiquitin-like modifier-activating enzyme 5
A_71_P110278	AK061178	LOC4332206	OSNPB_03024080 1	-2.7	4.6	elongation factor 1-alpha-like
A_71_P117528	AK064179	LOC4340325	OSNPB_06018410 0	-2.7	4.6	B3 domain-containing protein Os02g0598200-like
A_71_P119501	AK065696	LOC4343831	OSNPB_07060260 0	-2.7	4.6	Uncharacterized
A_71_P118242	AK069889	LOC4342267	OSNPB_07011900 0	-2.7	4.6	Uncharacterized
A_71_P124967	AK072582	LOC4349984	OSNPB_11019460 0	-2.7	4.6	protein MAIN-LIKE 2
A_71_P124115	AK106467	LOC4348087	OSNPB_10014190 0	-2.7	4.6	Uncharacterized
A_71_P124066	AK107022	LOC4348241	OSNPB_10019350 0	-2.7	4.6	17kDa alpha-amylase/trypsin inhibitor 2-like
A_71_P110063	AK058803	LOC4332352	OSNPB_03026580	-2.7	4.4	Uncharacterized
A_71_P107096	AK066613	LOC4330727	OSNPB_02074830 0	-2.7	4.4	serine/arginine repetitive matrix protein 1
A_71_P105265	AK069956	LOC4330113	OSNPB_02064080 0	-2.7	4.4	ran-binding protein 1 homolog a

A_71_P121291	AK101010	LOC9266867	OSNPB_070683200	-2.7	4.4	NAC transcription factor 29
A_71_P126741	AK106509	LOC4351270	OSNPB_120106700	-2.7	4.4	Uncharacterized
A_71_P121378	AK108589	LOC4344743	OSNPB_080164100	-2.7	4.4	probable methyltransferase PMT19
A_71_P104421	AK109015	LOC107275248	OSNPB_020593400	-2.7	4.4	Uncharacterized
A_71_P109351	AK062506	LOC4331362	OSNPB_030111300	-2.7	4.4	probable phospholipid hydroperoxide glutathione peroxidase
A_71_P108529	AK062977	LOC4331483	OSNPB_030127900	-2.7	4.4	cyclin-dependent kinase A-2-like
A_71_P117690	AK068356	LOC4331210	OSNPB_020825500	-2.7	4.4	Bifunctionalaspartokinase/homoserine dehydrogenase 2, chloroplastic
A_71_P105792	AK068761	LOC4330225	OSNPB_020661800	-2.7	4.4	mitochondrial proton/calcium exchanger protein
A_71_P103675	AK073433	LOC4325382	OSNPB_010957200	-2.7	4.4	Uncharacterized
A_71_P109785	AK099818	LOC4332656	OSNPB_030317000	-2.7	4.4	auxin transporter-like protein 1
A_71_P115818	AK103068	LOC4340349	OSNPB_060187000	-2.7	4.4	dihydroceramide fatty acyl 2-hydroxylase FAH2
A_71_P128158	AK110434	LOC4339717	OSNPB_050579900	-2.7	4.4	auxilin-related protein 1
A_71_P110945	AK058848	LOC4335799	OSNPB_040414700	2.5	6.0	photosystem I subunit O
A_71_P100324	AK065125	LOC4325653	OSNPB_010185200	2.5	6.0	beta-1,4-mannosyl-glycoprotein 4-beta-Nacetylglucosaminyltransferase
A_71_P105147	AK067722	LOC9267259	OSNPB_020526500	2.5	6.0	rho GTPase-activating protein 5
A_71_P104323	AK068122	LOC4331210	OSNPB_020825500	2.5	6.0	Uncharacterized
A_71_P110156	AK073459	LOC4333085	OSNPB_030409100	2.5	6.0	Uncharacterized
A_71_P112354	AK101902	LOC4335831	OSNPB_040420900	2.5	6.0	Uncharacterized
A_71_P110583	AK105818	LOC4332538	OSNPB_030296400	2.5	6.0	probable carboxylesterase 15
A_71_P106058	AK109318	LOC4329438	OSNPB_020506500	2.5	6.0	RNA-binding protein CP29B, chloroplastic
A_71_P123431	AK069758	LOC4348063	OSNPB_100136200	2.6	5.2	mitogen-activated protein kinase kinasekinase 5
A_71_P126492	AK072652	LOC4351897	OSNPB_120254400	2.6	5.2	Uncharacterized
A_71_P123717	AK100196	LOC4325457	OSNPB_010143100	2.6	5.2	mitochondrial substrate carrier family protein B
A_71_P118094	AK101955	LOC4343623	OSNPB_070565300	2.6	5.2	monothiol glutaredoxin-S2-like
A_71_P107503	AK103085	LOC4334311	OSNPB_030780800	2.6	5.2	calcium-dependent protein kinase 21-like
A_71_P119592	AK109447	LOC4343868	OSNPB_070608400	2.6	5.2	gallate 1-beta-glucosyltransferase
A_71_P114630	AK111471	LOC4338289	OSNPB_05028050	2.6	5.2	soluble inorganic pyrophosphatase

			0			
A_71_P110290	AK060019	LOC4332213	OSNPB_03024160 0	2.6	4.7	Uncharacterized
A_71_P107682	AK061464	LOC4331811	OSNPB_03017750 0	2.6	4.7	Uncharacterized
A_71_P124888	AK063652	LOC9270608	OSNPB_11053340 0	2.6	4.7	exosome complex component RRP41-like
A_71_P104586	AK064473	LOC4328332	OSNPB_02015300 0	2.6	4.7	DNA polymerase alpha subunit B
A_71_P119866	AK069066	LOC4346248	OSNPB_08054920 0	2.6	4.7	dehydrodolichyl diphosphate synthase 6
A_71_P123084	AK069924	LOC4348749	OSNPB_10044610 0	2.6	4.7	bromodomain-containing factor 2
A_71_P118954	AK070767	LOC4342293	OSNPB_07012290 0	2.6	4.7	probable alkaline/neutral invertase F
A_71_P103200	AK071060	LOC4325828	OSNPB_01094620 0	2.6	4.7	Unknown expressed protein
A_71_P111340	AK058975	LOC4335998	OSNPB_04045050 0	2.6	4.9	Uncharacterized
A_71_P125379	AK060118	LOC4349805	OSNPB_11015330 0	2.6	4.9	Unknown expressed protein
A_71_P104150	AK065136	LOC4329854	OSNPB_02059510 0	2.6	4.9	methylcrotonoyl-CoA carboxylase subunit alpha, mitochondrial-like
A_71_P111210	AK100967	LOC4335200	OSNPB_04022160 0	2.6	4.9	Uncharacterized
A_71_P113166	AK101116	LOC4336249	OSNPB_04049150 0	2.6	4.9	protein NRT1/ PTR FAMILY 4.5
A_71_P123021	AK103655	LOC4349117	OSNPB_10051640 0	2.6	4.9	Uncharacterized
A_71_P118139	AK107633	LOC4342730	OSNPB_07021670 0	2.6	4.9	Uncharacterized
A_71_P128030	AK110267	LOC9266867	OSNPB_07068320 0	2.6	4.9	NAC transcription factor 29
A_71_P120556	AK062863	LOC4345581	OSNPB_08041690 0	2.7	5.1	K(+) efflux antiporter 5
A_71_P117434	AK063377	LOC4329688	OSNPB_02056240 0	2.7	5.1	cyclin-dependent kinase A-2-like
A_71_P107424	AK063885	LOC112938227	OSNPB_03027670 0	2.7	5.1	Uncharacterized
A_71_P126067	AK065165	LOC4352741	OSNPB_12060580 0	2.7	5.1	BURP domain-containing protein 3-like
A_71_P114418	AK099313	LOC4339617	OSNPB_05056360 0	2.7	5.1	Uncharacterized
A_71_P104020	AK104474	LOC4331018	OSNPB_02079760 0	2.7	5.1	Uncharacterized
A_71_P107567	AK109412	LOC4332957	OSNPB_03037660 0	2.7	5.1	PHD finger protein ALFIN-LIKE 9-like
A_71_P128033	AK110273	LOC9269069	OSNPB_12010530 0	2.7	5.1	protein CHUP1, chloroplastic
A_71_P101793	AK111757	LOC4325072	OSNPB_01086650 0	2.7	4.8	delta(14)-sterol reductase
A_71_P111748	AK062772	LOC4336627	OSNPB_04055630 0	2.7	5.0	Oryza sativa glutathione peroxidase 1 (GPX1)

A_71_P107943	AK068484	LOC4333501	OSNPB_030626700	2.7	5.0	Uncharacterized
A_71_P107609	AK068746	LOC4333878	OSNPB_030710600	2.7	5.0	probable lipid phosphate phosphatase beta
A_71_P124577	AK072924	LOC4350916	OSNPB_110614900	2.7	5.0	transcription initiation factor TFIID subunit 15b
A_71_P113689	AK099719	LOC9267958	OSNPB_050143500	2.7	5.0	YTH domain-containing family protein 2
A_71_P119849	AK101404	LOC4344441	OSNPB_080104800	2.7	5.0	arginase 1, mitochondrial-like
A_71_P111324	AK109889	LOC4336181	OSNPB_040480900	2.7	5.0	Unknown expressed protein
A_71_P121341	AK058477	LOC4345657	OSNPB_080434300	2.8	5.2	malate dehydrogenase, chloroplastic
A_71_P122196	AK068061	LOC4347311	OSNPB_090465600	2.8	5.2	Uncharacterized
A_71_P106957	AK072724	LOC4329681	OSNPB_020558500	2.8	5.2	Uncharacterized
A_71_P112363	AK073418	LOC4335786	OSNPB_040412900	2.8	5.2	Uncharacterized
A_71_P118271	AK101648	LOC4343803	OSNPB_070598300	2.8	5.2	zinc finger CCHC domain-containing protein 10
A_71_P117346	AK108060	LOC4331157	OSNPB_020818900	2.8	5.2	F-box protein SKIP23
A_71_P128236	AK110559	LOC9270256	OSNPB_010698900	2.8	5.2	nascent polypeptide-associated complex subunit alpha-like protein 2
A_71_P128274	AK110618	LOC4344309	OSNPB_070682000	2.8	5.2	protein PYRICULARIA ORYZAE RESISTANCE 21-like
A_71_P113288	AK067481	LOC4337526	OSNPB_050101400	2.8	5.2	TNF receptor-associated factor 6
A_71_P124567	AK070884	LOC4349916	OSNPB_110175400	2.8	5.2	NAC domain-containing protein 48-like
A_71_P110906	AK100347	LOC4335990	OSNPB_040449500	2.8	5.2	protein FLX-like 2
A_71_P113574	AK100817	LOC4335199	OSNPB_040221600	2.8	5.2	Uncharacterized
A_71_P125669	AK101496	LOC9272227	OSNPB_120467300	2.8	5.2	transducin beta-like protein 3
A_71_P112718	AK102284	LOC4337089	OSNPB_040629300	2.8	5.2	probable isoprenylcysteine alpha-carbonyl methylesterase ICMEL1
A_71_P117818	AK109158	LOC4343876	OSNPB_070611700	2.8	5.2	rust resistance kinase Lr10
A_71_P103769	AK110526	LOC4326871	OSNPB_010542700	2.8	5.2	Uncharacterized
A_71_P100337	AK071475	LOC4326040	OSNPB_010121100	3.1	6.6	ankyrin repeat protein SKIP35
A_71_P109704	AK060233	LOC4333169	OSNPB_030428800	3.1	7.7	Uncharacterized
A_71_P120608	AK059773	LOC9268297	OSNPB_080470200	3.3	5.2	alpha carbonic anhydrase 7
A_71_P113554	AK061590	LOC4339442	OSNPB_050535700	3.3	5.2	polyadenylate-binding protein RBP45
A_71_P120282	AK063695	LOC4344519	OSNPB_08011680	3.3	5.2	exosome complex component RRP41-

			0			like
A_71_P109622	AK066412	LOC4334569	OSNPB_030816900	3.3	5.2	potassium transporter 22-like
A_71_P111475	AK068782	LOC4336282	OSNPB_040496800	3.3	5.2	Uncharacterized
A_71_P119110	AK069186	LOC4343863	OSNPB_070607700	3.3	5.2	Uncharacterized
A_71_P101086	AK069974	LOC4327340	OSNPB_010198900	3.3	5.2	heavy metal-associated isoprenylated plant protein 7
A_71_P125732	AK101059	LOC4352458	OSNPB_120548100	3.3	5.2	condensin-2 complex subunit D3
A_71_P104256	AK107997	LOC4331157	OSNPB_020818900	3.3	5.2	Uncharacterized
A_71_P120258	AK059812	LOC4344519	OSNPB_080116800	4.5	4.0	Uncharacterized
A_71_P120991	AK065015	LOC4344674	OSNPB_080152700	4.8	9.8	sphingoid long-chain bases kinase 1
A_71_P111306	AK105252	LOC4333169	OSNPB_030428800	5.8	7.4	Uncharacterized
A_71_P105174	AK073100	LOC4330420	OSNPB_020698800	8.5	7.9	probable WRKY transcription factor 14
A_71_P118665	AK107155	LOC4344172	OSNPB_070659800	8.5	7.9	E3 ubiquitin-protein ligase DIS1-like
A_71_P110167	AK100651	LOC4344172	OSNPB_070659800	12.5	4.0	E3 ubiquitin-protein ligase DIS1-like
A_71_P116544	AK111324	LOC4341136	OSNPB_060507300	6.3	4.8	BTB/POZ domain-containing protein POB1
A_71_P110549	AK072820	LOC4332739	OSNPB_030332700	12.5	5.8	ABC transporter I family member 6, chloroplastic
A_71_P102603	AK100208	LOC4327679	OSNPB_010707500	9.4	6.7	bHLH transcription factor

Functional Characterization of drought-responsive genes

The differentially expressed genes were classified into functional categories. The functional annotation of these genes is based on sequences which match to other sequences in the GenBank using BLAST analysis. The result is set with the threshold of expectation value less than 10-10. Among the 171 differentially expressed transcripts, 57 belong to genes with unknown functions. The dissection of the expressed gene profile of tef under drought stress showed that most of the transcripts (93) were down-regulated (Figure 4). On the other hand, 77 transcripts were up-regulated under drought stress. Those differentially expressed genes between drought-stressed and well-irrigated tef root plant (77 up-regulated and 93 down-regulated) were identified by Linear Models for Microarray (LIMMA) (adjusted p-value ≤ 0.05; with fold change (FC) of |2|).

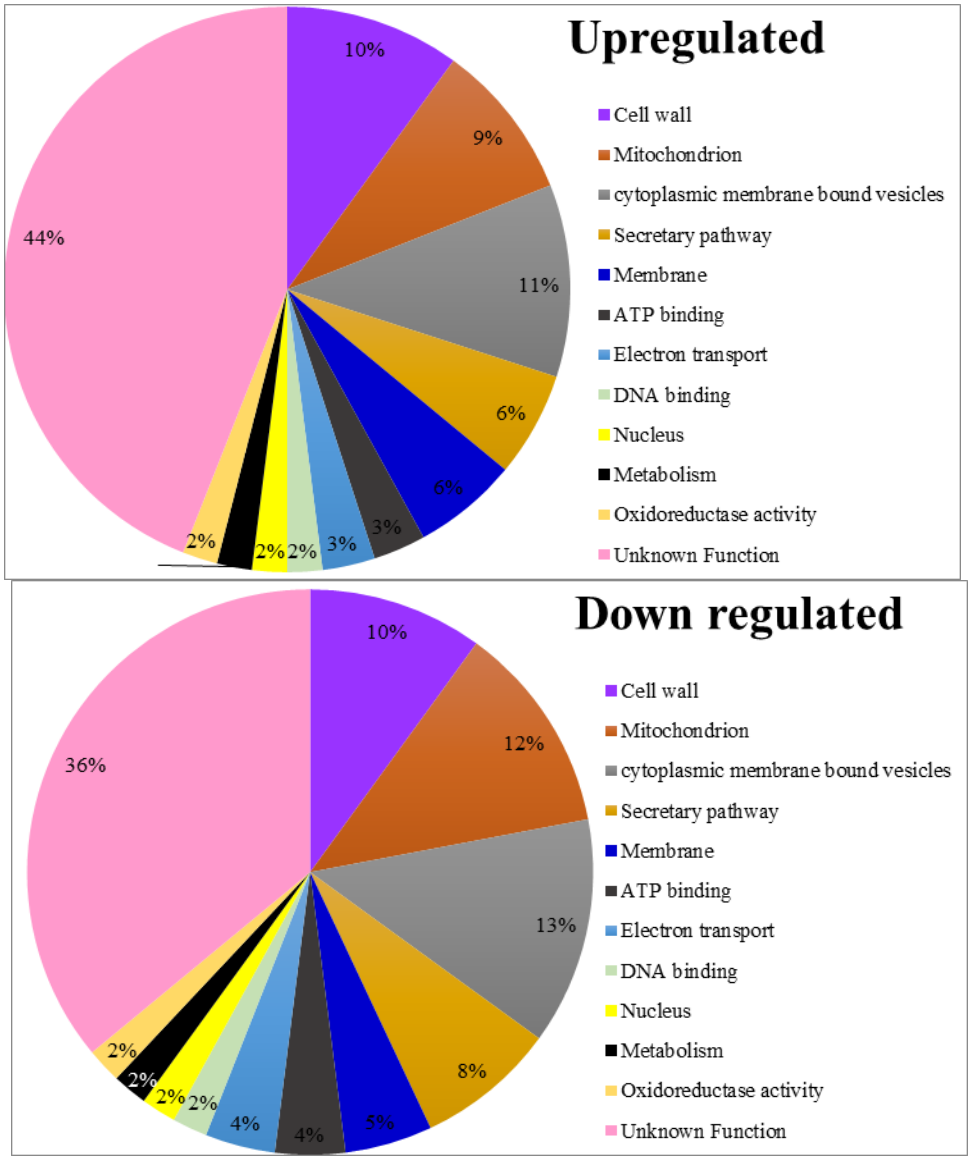

Figure 5. Distribution of drought responsive genes in E. tef for their functional classes. Percentage of drought responsive genes in the various functional categories; Up-regulated (top) and Down- regulated (bottom).

The resulting unregulated and down-regulated genes were further analyzed using the Gene Ontology (GO) Enrichment analysis to identify their molecular function. The majority of the transcripts belong to the unknown function 44% and 36% for up-regulated and down-regulated genes, respectively. The rest were categorized into cell wall (10%), Mitochondrion (9% and 12%), cytoplasm membrane-bound vesicles (11% and 13%), secretary pathway (6% and 8%), membrane (5% and 6%), ATP binding (3% and 4%), electron transport (3% and 4%), cellular process (21%), localization (7%), DNA binding (2%), Nucleus (2%), metabolism(2%), and Oxidoreductase activity (2%), were for up-regulated and down-regulated genes, respectively (Figure5).

RT-PCR, Real-Time Quantitative PCR and Northern blot analysis of highly differentially expressed transcript

Preliminary assessment of gene expression patterns under the normal control (well-irrigated) and drought stress in tef root (for 2, 4, 6, and 8) was performed for WRKY gene (Table 2) by quantitative RT-PCR, Real-time Quantitative PCR and Northern blot (Figure 6). The expression patterns under well irrigated and drought stress conditions differed significantly (LSD0.05 = 0.49). This gene was not expressed at all under the well-irrigated condition as evidenced in expression analysis.. This implies the gene was significantly induced by drought in the roots.

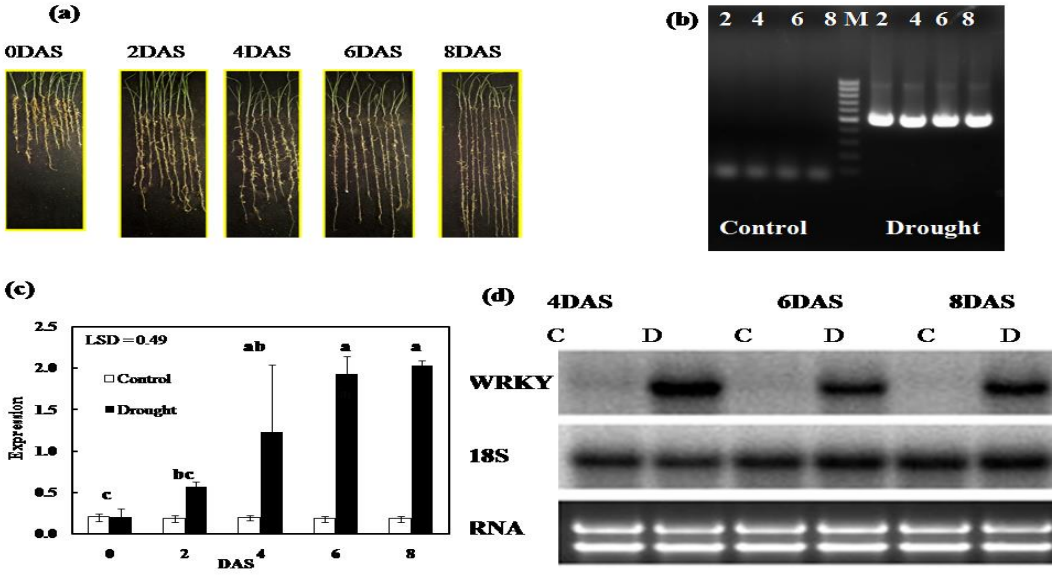

Figure 6. (a) The elongation of tef root (scale bar 35 cm) under drought stress compared to control from 0 to 8 DAS (days after stress). (b) RT-PCR analysis of tef's root WRKY gene after treatment for 2,4,6 and 8 days under drought stress. (c) Effect of drought stress on gene expression of WRKY in roots of tef. (d) Effect of drought stress on WRKY gene in tef root cells. Total RNAs were isolated from tef root which grow under drought stress for 4, 6 and 8 days. Total RNAs (10 µg each) were electrophoreses on an agarose gel, transferred onto a membrane and were probed with 32P-labeled isoform specific DNA fragments. The lower panel shows the quantification of ethidium bromide-stained total RNA after 4, 6 and 8 days after drought stress. Symbols, C and D indicate the well irrigated and drought stressed sample, respectively. that the levels of the TDFs are increased or not affected by the treatments, respectively. To show equal amount of RNA for all used for all experiment, 18S ribosome cDNA is control.

Discussion

Well irrigated and drought-stressed Kaye Murri showed significant variation in terms of shoot and root RWC, OP and OA suggest that drought stress tolerance mechanism by OA is operating on tef.

The drought-stressed plants had higher OA value and elongated root length, which indicated that some drought tolerance mechanism is operating by OA and deep root system under drought stress. This implies that the two traits can be studied at the molecular level to elucidate the tolerant mechanism of tef under drought stress. The increased seminal root length in tef under the drought stress is due to

the shift in elongation of the shoot as compared to the well-irrigated leaf sample (Figure 3).

To unravel the transcripts related to the elongation of the root in tef, rice microarray chips with the known gene was used in this experiment. Rice is a model plant where extensive studies related to drought has been carried out (Moon and Jung, 2014; Moon *et al*., 2014a, 2018; Ramamoorthy *et al*., 2008). Multiple whole-genome sequences of rice and transcription studies and other molecular tools are available for this crop. Tef is one of the most drought-tolerant cereals, providing a useful platform to understand the mystery of root elongation under drought stress. Since many of the monocot genomes had high synteny (Choe *et al*., 2018), it is feasible to use rice chips to do hybridization with tef RNAs. However, from the hybridization of tef and rice transcripts, only 171 genes are differentially regulated. This might be the low homology of the rice orthologs to tef RNA.

Several ABC transporter family members are up-regulated in tef root under drought stress. This transcript is essential in transporting compounds which are important in drought adaptation (Lane *et al*., 2016). The larger number of ABC transporter genes are important in their ability to sequester and transport foreign chemicals and compound to protect the plant under drought stress (Hwang *et al*., 2016; Moon et al., 2014b). Basic helix–loop–helix (BHLH) transcription factor is also up-regulated in drought-stressed tef root. This transcription factor is responsible for the initiation of root development in plants (Schlereth *et al*., 2010). This involves the embryonic root signal for initiation of root elongation in tef root under drought stress.

However, WRKY transcription factor 14 is highly up regulated under drought stress. The role of WRKY transcription factors has been studied by many researchers on many crop plants under abiotic stress (Dong *et al*., 2003; Eulgem and Somssich, 2007; Eulgem *et al*., 2000; Mangelsen *et al*., 2008; Pandey and Somssich, 2009; Ren *et al*., 2010; Ross et al., 2007; Rushton *et al*., 2010; Shen *et al*., 2012). The expression of this transcription factor contributes to the various signaling pathways in plants. The translated protein regulates different functions as a negative or positive regulator. The up-regulation of this gene under drought stress and its confirmation by real-time and the Northern blot analysis indicate that it is involved in various regulatory functions.

We also observed that there is the down regulation of important transcription factors like CCHC-type zinc finger protein, GTPase-activating protein, BTB/POZ, and carbonic anhydrase protein under the drought-stressed root of tef. Gene regulation involves regulation of cis-acting transcription factors like CCHC both in DNA and RNA (Yang *et al*., 2017). The GAF BTB/POZ domain has also contributed to interactions with non-BTB/POZ proteins which reduced programmed cell death, and is an indication of the negative regulation of plant immune pathway (Orosa *et al*., 2017)**.** Mitochondrial genes were also down-regulated (Table 1). The biosynthesis and morphological regulation of mitochondria were highly affected by the gene carnitine (Piemontese *et al*., 2017). This protein was involved in the metabolic pathways to regulate plants under drought stress (Rao *et al*., 2017). GTP binding proteins are up-regulated under drought stress and are involved in the root hair formation (Wang *et al*., 2016). In tef root, these genes were up-regulated and the morphology of tef roots under drought stress had less root hair development (Figure 1, Figure 6). Carbonic anhydrase plays a major role in all photosynthetic organism (DiMario et al., 2017) and is involved in the synthesis of lipid molecules in the plant (Ludwig, 2016). It seems that multiple genes of the Carbonic anhydrase are involved in the conversion of lipid in the root cell to facilitate the energy biosynthesis under drought stress; thus, facilitating the root elongation process by fueling for an energy source.

The molecular function of down-regulated genes includes transcription factor, hydrolyzing activity, RNA binding, transmembrane transporter, enzyme inhibiting, oxidoreductase and DNA binding activity (Table 2). TCP encodes plant-specific transcription factors like Transcription factor PCF8. Researches indicated that the down-regulation of PCF8 results in an increased tolerance towards abiotic stress (Yang *et al*., 2013). Membrane-anchored ubiquitin-fold

protein 3 is involved in all biological process of eukaryotic plants. Mostly, E3 ligase binds to this protein and is involved in the regulation, production, and signaling of plant hormones (Nagels Durand *et al*., 2016). BTB/POZ PROTEIN 1 is involved in the regulation of crown rootless gene (CRL3) (Yu *et al*., 2016). The fact that this gene is down regulated in tef indicates its major involvements in delaying the crown root formation while facilitating seminal root elongation. Thus, the morphology of tef root is elongated seminal root with a few crown root formations.

Conclusion

Tef responds to drought by elongating the seminal root. One hundred seventy-six (176) differentially expressed transcripts were identified in the roots of the tef plants, under drought and well-irrigated conditions. The differentially regulated transcriptsconfirm the presence of key regulatory elements controlling the elongation of root related to the drought response. Extensive responsive transcripts are up-regulated under drought stress to sense the amount of water in the soil for proper growth and development. Transcripts linked to biosynthesis are expressed in response to drought stress. Thus, this transcriptome analysis allowed us to find putative targets for further functional investigation of tef root under drought stress. Further studies are essential to characterize the molecular functions of root and leaf transcripts under drought stress. Thus, the information would give us a better understanding to unravel the adaptation of tef under drought specific environmental conditions.

Acknowledgments

This research was supported by Japan Ministry of Agriculture, Education and Culture project "crop breeding." We would like to extend our acknowledgment to the ministry.

References

Abraha M., Shimelis H, Laing M, and Assefa K (2016). Performance of Tef [(Zucc.) Trotter] Genotypes for Yield and Yield Components Under Drought-Stressed and Non-Stressed Conditions. Crop Sci. *56*, 1799–1806.

Admas S, and Belay G (2011). Drought-resistance traits variability in *Eragrostis tef* X *Eragrostis pilosa* recombinant inbred lines. Afr. J. Agric. Res. *6*, 3755–3761.

Assefa K, Yu JK, Zeid M, Belay G, Tefera H, and Sorrells, ME (2011). Breeding tef [Eragrostistef (Zucc.) trotter]: conventional and molecular approaches. Plant Breed. *130*, 1–9.

Ayele M (1999). Genetic diversity in tef (*Eragrostis tef* (zucc) Trotter) for osmotic adjustment, root traits, and Amplified Fragment Length Polymorphism. Texas Tech University.

Belay G, Tefera H, Getachew A, Assefa K, and Metaferia G (2008). Highly client-oriented breeding with farmer participation in the Ethiopian cereal tef *[Eragrostis tef* (Zucc.) Trotter]. Afr. J. Agric. Res. *3*, 022–028.

BelayG, Zemede A, Assefa K, Metaferia G, and Tefera H (2009). Seed size effect on grain weight and agronomic performance of tef *[Eragrostis tef* (Zucc.) Trotter]. Afr. J. Agric. Res. *4*, 836–839.

Cannarozzi G, Plaza-Wüthrich S, Esfeld K. Larti S, Wilson YS, Girma D, de Castro E, Chanyalew S, Blösch R, FarinelliL,. (2014). Genome and transcriptome sequencing identifies breeding targets in the orphan crop tef (*Eragrostis tef*). BMC Genomics *15*, 581.

Choe, J., Kim, J.-E., Lee, B.-W., Lee, J.H., Nam, M., Park, Y.-I., and Jo, S.-H. (2018). A comparative synteny analysis tool for target-gene SNP marker discovery: connecting genomics data to breeding in Solanaceae. Database *2018*.

Degu HD, Ohta M, and Fujimura T (2008). Drought Tolerance of *Eragrostis tef* and Development of Roots. Int. J. Plant Sci. *169*, 768–775.

Degu, HD, and Fujimura T (2010). Mapping QTLs Related to Plant Height and Root Development of *Eragrostis tef* under Drought. J. Agric. Sci. *2*, 62.

DiMario RJ, Clayton H, Mukherjee A, Ludwig M, and Moroney JV (2017). Plant Carbonic

Anhydrases: Structures, Locations, Evolution, and Physiological Roles. Mol. Plant *10*, 30–46.

Dong J, Chen C, and Chen Z (2003). Expression profiles of the Arabidopsis WRKY gene super family during plant defense response. Plant Mol. Biol. *51*, 21–37.

Eulgem T, and Somssich IE (2007). Networks of WRKY transcription factors in defense signaling. Curr. Opin. Plant Biol. *10*, 366–371.

Eulgem T, Rushton PJ, Robatzek S, and Somssich IE (2000). The WRKY superfamily of plant transcription factors. Trends Plant Sci. *5*, 199–206.

Hailesillasie H, Araya A., Habtu S, Meles KG, Gebru G, Kisekka I, Girma A, HadguKM, and Foste, AJ (2016). Exploring optimal farm resources management strategy for Quncho-teff (*Eragrostis tef* (Zucc.) Trotter) using AquaCrop model. Agric. Water Manag. *178*, 148–158.

Hwang JU, Song WY, Hong D, Ko D, Yamaoka Y, Jang S, Yim S, Lee E, Khare D, Kim K, (2016). Plant ABC Transporters Enable Many Unique Aspects of a Terrestrial Plant's Lifestyle. Mol. Plant *9*, 338–355.

Lane TS, Rempe CS, Davitt J, Staton ME, Peng Y, Soltis D, Melkonian M, Deyholos M, Leebens Mack JH, Chase M, (2016). Diversity of ABC transporter genes across the plant kingdom and their potential utility in biotechnology. BMC Biotechnol. *16*, 47.

Ludwig M (2016). Evolution of carbonic anhydrase in C 4 plants. Curr. Opin. Plant Biol. *31*, 16–22.

Mangelsen E, Kilian J, Berendzen KW, Kolukisaoglu ÜH., Harter K, Jansson C, and Wanke D(2008). Phylogenetic and comparative gene expression analysis of barley (*Hordeum vulgare*) WRKY transcription factor family reveals putatively retained functions between monocots and dicots. BMC Genomics *9*, 194.

Maruyama K, Yamaguchi-Shinozaki K., and Shinozaki K. (2014). Gene expression profiling using DNA microarrays. Arab. Protoc. 381–391.

McCouch SR., Symbolization C (Committee on G., Linkage, N. and, and Cooperative) RG (2008). Gene Nomenclature System for Rice. Rice *1*, 72–84.

Mi H, Poudel S, Muruganujan A., Casagrande JT., and Thomas PD (2016). PANTHER version 10: expanded protein families and functions, and analysis tools. Nucleic Acids Res. *44*, D336-342.

Moon S, and Jung K.H. (2014). Genome-wide expression analysis of rice ABC transporter family across spatio-temporal samples and in response to abiotic stresses. J. Plant Physiol. *171*, 1276–1288.

Moon S, Jung, K.H, and others (2014a). Genome-wide expression analysis of rice ABC transporter family across spatio-temporal samples and in response to abiotic stresses. J. Plant Physiol. *171*, 1276–1288.

Moon, S, Jung, KH, and others (2014b). Genome-wide expression analysis of rice ABC transporter family across spatio-temporal samples and in response to abiotic stresses. J. Plant Physiol. *171*, 1276–1288.

Moon S, Chandran AN, An G, Lee C, and Jung, KH. (2018). Genome-wide analysis of root hair-preferential genes in rice. Rice *11*, 48.

Smyth GK., Ritchie M, Thorne N, and Wettenhall J (2005). LIMMA: linear models for microarray data. In Bioinformatics and Computational Biology Solutions Using R and Bioconductor. Statistics for Biology and Health.

Nagels ., Pauwels L, and Goossens A. (2016). The Ubiquitin System and Jasmonate Signaling. Plants *5*, 6.

Orosa B, He Q, Mesmar J, Gilroy, EM, McLellan H, Yang C, Craig A, Bailey M, Zhang C, Moore JD, (2017). BTB-BACK Domain Protein POB1 Suppresses Immune Cell Death by Targeting Ubiquitin E3 ligase PUB17 for Degradation. PLOS Genet. *13*, e1006540.

Pandey SP, and Somssich IE (2009). The role of WRKY transcription factors in plant immunity. Plant Physiol. *150*, 1648–1655.

Piemontese L, Cerchia C, Laghezza A, Ziccardi P, SblanoS, Tortorella P, Iacobazzi V, Infantino V, Convertini P, Dal Piaz, F, (2017). New diphenylmethane derivatives as peroxisome proliferator-activated receptor alpha/gamma dual agonists endowed with anti-proliferative effects and mitochondrial activity. Eur. J. Med. Chem. *127*, 379–397.

Plaza S, Cannarozzi GM, and Tadele Z (2013). Genetic and phenotypic diversity in selected genotypes of tef [Eragrostistef (Zucc.)] Trotter. Afr. J. Agric. Res. *8*, 1041–1049.

Ramamoorthy R. Jiang, S, Kumar N, Venkatesh PN, and Ramachandran S (2008). A Comprehensive Transcriptional Profiling of the WRKY Gene Family in Rice Under Various Abiotic and Phytohormone Treatments. Plant Cell Physiol. *49*, 865–879.

Rao RP, Salvato F, Thal B, Eubel H, Thelen JJ, and Møller IM (2017). The proteome of higher plant mitochondria. Mitochondrion *33*, 22–37.

Ren X, Chen Z, Liu Y, Zhang H, Zhang M, Liu Q, Hong X, Zhu JK, and Gong Z (2010). ABO3, a WRKY transcription factor, mediates plant responses to abscisic acid and drought tolerance in Arabidopsis. Plant J. *63*, 417–429.

Ritchie ME, Phipson B, Wu D, HuY, Law CW, Shi W, and Smyth GK. (2015). limma powers differential expression analyses for RNA-sequencing and microarray studies. Nucleic Acids Res. 43,e47.

Ross CA, Liu Y, and Shen QJ (2007). The WRKY gene family in rice (Oryza sativa). J. Integr. Plant Biol. *49*, 827–842.

Rushton PJ, Somssich IE, Ringler P, and She, QJ (2010). WRKY transcription factors. Trends Plant Sci. *15*, 247–258.

Sato Y, Takehisa H, Kamatsuki K., Minami H, Namiki N, Ikawa H, Ohyanagi H, Sugimoto K, Antonio BA, and Nagamura, Y (2013). RiceXPro Version 3.0: expanding the informatics resource for rice transcriptome. Nucleic Acids Res. *41*, D1206–D1213.

Schlereth A, Möller B, Liu, W, Kientz M, Flipse J, Rademacher EH, Schmid M, Jürgens G, and Weijers D (2010). MONOPTEROS controls embryonic root initiation by regulating a mobile transcription factor. Nature *464*, 913–916.

Shen H, Liu C, Zhang Y, Meng X, Zhou X, Chu C, and Wang X (2012). OsWRKY30 is activated by MAP kinases to confer drought tolerance in rice. Plant Mol. Biol. *80*, 241–253.

SU SL, Singh DN, and Baghini MS (2014). A critical review of soil moisture measurement. Measurement *54*, 92–105.

R Core Team (2018). R: A language and environment for statistical computing. R Foundation for Statistical Computing, Vienna, Austria. URL URL https://www.R-project.org/

Wang H, Lan P, and Shen RF (2016). Integration of transcriptomic and proteomic analysis towards understanding the systems biology of root hairs. Proteomics. 16: 877-893.

Yang C, Li D, Mao D, Liu X, Ji C, Li X, Zhao X, Cheng Z, Chen C, and Zhu L (2013). Overexpression of microRNA319 impacts leaf morphogenesis and leads to enhanced cold tolerance in rice (*Oryza sativa* L.): Rice miR319 and cold response. Plant Cell Environ. *36*, 2207–2218.

Yang F, Hsu P, Lee SD, Yang W, Hoskinson D, Xu W, Moore C, and Varani G (2017). The C terminus of Pcf11 forms a novel zinc-finger structure that plays an essential role in mRNA 3'-end processing. RNA *23*, 98–107.

Yu, Gutjahr Li C, and Hochholdinger F (2016). Genetic control of lateral root formation in cereals. Trends in Plant Sci. *21*, 951–961.